DØ Note 6286-CONF

Search for the standard model Higgs boson in the $\tau\tau\mu + X$ final state in 7.0 fb^{-1} of $p\bar{p}$ collisions at $\sqrt{s} = 1.96$ TeV

The DØ Collaboration
URL http://www-d0.fnal.gov
(Dated: March 5, 2012)

We present a search for the production of the standard model Higgs boson studying the final state $\tau\tau\mu + X$ using data collected with the D0 detector at the Fermilab Tevatron $p\bar{p}$ collider and corresponding to an integrated luminosity $L = 7.0$ fb^{-1}. No significant excess of data is observed over the background expectaction and limits are set on the cross section relative to its standard model prediction. The observed (expected) limit for a Higgs boson with a mass of 120 GeV is 10.7 (14.2) times the SM cross section.

Preliminary Results for Winter 2012 Conferences

I. INTRODUCTION

The standard model (SM) of particle physics has only one element that remains undiscovered, the Higgs Boson. The existence of this particle was suggested in 1964 as part of the mechanism introduced to provide mass to the weak bosons without breaking unitarity. The Higgs boson has been searched for almost continuously since but as yet no experimental evidence has been seen. As the analysis methods and detectors searching for it improve, it is being slowly constrained to a smaller region of mass. Strong limits on the Higgs boson have been set at a number of experiments, noticeably at LEP which set limits at 95% confidence level on all masses below 114.4 GeV [1], and from the Tevatron where the combined limits from DØ and CDF have excluded masses between 156 and 177 GeV [2]. Most recently, at the LHC the limits from the CMS [3] and ATLAS [4] detectors have excluded a large region at 95% confidence level leaving a narrow allowed mass region between 116 and 127 GeV. Theoretical considerations greatly restrict the likelihood of the SM having a mass greater than 500 GeV.

Although the specific mass of the Higgs boson is not predicted, its relative coupling strengths to the different quarks and leptons are, and it is predicted to couple most strongly to the heaviest particles. For leptonic decay modes one expects the largest coupling to the tau lepton, the heaviest of the leptons.

In this paper we present a search for the standard model Higgs boson decaying leptonically to a $\tau\tau\mu$ final state. This is based on data collected with the D0 detector at the Fermilab Tevatron Collider and corresponds to an integrated luminosity of up to 7.0 fb^{-1}. We require that there is at least one μ and two hadronic τ leptons in the final state. This analysis will be complementary with similar DØ analyses looking for a SM Higgs boson decaying leptonically to $\mu\mu e$ and $ee\mu$ final states [5]. These analyses are in general referred to as trilepton analyses.

The dominant Higgs boson decays to which this analysis is sensitive are $H \to \tau\tau$, $H \to \mu\mu$, $H \to WW$ and $H \to ZZ$. At the Tevatron the primary SM Higgs production mechanism is gluon-gluon fusion $gg \to H$, (ggf). The associated production of a Higgs with a W or Z boson, WH and ZH, also contributes, in addition to a small contribution from vector boson fusion $VV \to H$, (VBF). This analysis is expected to be mainly sensitive to a Higgs produced through associated production due to the requirement on a third lepton.

II. EVENT SELECTION

The D0 detector [6] comprises tracking detectors and calorimeters. Silicon microstrip detectors and a scintillating fiber tracker are used to reconstruct charged particle tracks within a 1.9 T solenoid. The uranium/liquid-argon calorimeters used to measure particle energies consist of electromagnetic (EM) and hadronic sections. Muons are identified by combining tracks in the central tracker with patterns of hits in the muon spectrometer. Events are required to pass triggers that select at least one muon candidate.

All background processes are simulated using Monte Carlo (MC) event generators, except for the instrumental background in which an event originating from W+jets or from multijet production is selected in the final sample because one or more of the jets are identified as τ or μ. The $Z/\gamma^* \to \ell^+\ell^-$, and $t\bar{t}$ processes are generated using ALPGEN [7] with showering and hadronization provided by PYTHIA [8]. The instrumental background is determined from data. Diboson production (WW, WZ, and ZZ) and signal events are simulated using PYTHIA.

Samples were produced for the production of a standard model Higgs in the following modes: a SM Higgs boson produced in association with a W and Z boson, a Higgs produced by vector boson fusion and the production of a Higgs via gluon-gluon fusion decaying to ZZ or WW final states. For all production processes, we simulate the decays $H \to WW$, $H \to ZZ$, $H \to \gamma\gamma$, $H \to ee$, $H \to \mu\mu$, $H \to \tau\tau$ and $H \to \gamma Z$ using HDEACY [9] to determine the mass-dependent branching ratios. The Higgs samples were produced in the mass range 100-200 GeV, at 5 GeV intervals.

The tau lepton decays are simulated with TAUOLA [10], which includes a full treatment of the tau polarization. All MC samples are processed through a GEANT [11] simulation of the detector. Data from random beam crossings are overlaid on MC events to account for detector noise and additional $p\bar{p}$ interactions. The simulated distributions are corrected for the dependence of the trigger efficiency in data on the instantaneous luminosity, and for differences between data and simulation in the reconstruction efficiencies and in the distribution of the longitudinal coordinate of the interaction point along the beam direction. Next-to-leading order (NLO) quantum chromodynamics calculations of cross sections are used to normalize the signal and the background contribution of diboson processes, and next-to-NLO calculations are used for all other processes.

Three types of tau lepton decays into hadrons (τ_h) are identified by their signatures: type 1 tau candidates consist of a calorimeter cluster, with one associated track and no additional sub-cluster in the EM section of the calorimeter. This signature corresponds mainly to $\tau^\pm \to \pi^\pm\nu$ decays. For type 2 tau candidates, an energy deposit in the EM calorimeter is required in addition to the type 1 signature, as expected for $\tau^\pm \to \pi^\pm\pi^0\nu$ decays. For type 3 tau candidates, a calorimeter cluster, with two or three associated tracks, with or without EM subclusters. This

corresponds mainly to the decays $\tau^{\pm} \to \pi^{\pm}\pi^{\pm}\pi^{\mp}(\pi^0)\nu$ (3-prong). The outputs of neural networks, one for each tau-type, designed to discriminate τ_h from jets, have to be $NN_\tau > 0.75$ for type 1 and 2 taus and $NN_\tau > 0.95$ for type 3 taus [12]. Their input variables are based on isolation variables for objects and on the spatial distribution of showers. We use the energy measurement in the calorimeter to define the transverse momentum of the τ.

We select events with at least one muon and at least two τ_h candidates. The muons must be isolated, both in the tracking detectors and in the calorimeters. Each event must have a reconstructed $p\overline{p}$ interaction vertex located within 60 cm of the nominal center of the detector along the beam axis. The pseudorapidity [13] of the selected muons, τ_1, and τ_2 must be $|\eta^{\mu}| < 1.6$ and $|\eta^{\tau_i}| < 1.5$, respectively, and for additional τ_h candidates we require $|\eta^{\tau}| < 2$. The transverse momenta must be $p_T^{\mu} > 15$ GeV and $p_T^{\tau_i} > 12.5$ GeV for type 1 or type 2 taus and $p_T^{\tau_i} > 15$ GeV for type 3 taus. All selected τ_h candidates and muons are required to be separated by $\Delta\mathcal{R}_{\mu\tau} > 0.5$, where $\Delta\mathcal{R} = \sqrt{(\Delta\phi)^2 + (\Delta\eta)^2}$ and ϕ is the azimuthal angle, and the two leading τ_h must be separated by $\Delta\mathcal{R}_{\tau_1\tau_2} > 0.7$. The sum of the charges of the highest-p_T muon, τ_1, and τ_2 is required to be $Q = \sum_{i=\mu,\tau_1,\tau_2} q_i = \pm 1$ as expected for signal. A cut on the missing transverse energy, $\not\!\!E_T > 22.5$ GeV is also required. In order to ensure orthogonality with the other trilepton analysis, the events which satisfy the selection criteria for the $\mu\mu e$ and $ee\mu$ final states are excluded from the sample considered here. Calorimeter jets are reconstructed from the energy deposited in the calorimeter cells using the Run II cone algorithm with a cone size of R = 0.5. Reconstructed jets are required to have $p_T > 15$ GeV and to be separated from muon and tau candidates by $\Delta\mathcal{R}_{jet\tau/\mu} > 0.5$. After all selections, the main background are from diboson production, instrumental backgrounds and $Z \to \tau^+\tau^-$, where an additional jet mimics a lepton.

TABLE I: Numbers of events in data, predicted background, and expected signal for $M = 120$ GeV, for all events at final selection and separated into bins of jet multiplicity.

	All bins	NJet = 0	NJet =1	NJet $\geq$ 2
Data	28	6	14	9
$Z \to \tau\tau$	9.19	2.17	4.06	2.96
$Z \to \mu\mu$	2.79	0.75	1.21	0.83
$Z \to ee$	0.94	0.15	0.63	0.16
$t\bar{t}$	1.41	0.08	0.36	0.7
Diboson	8.98	5.09	3.08	0.81
multijet & W+jet	6.82	0.12	0.32	6.38
Total Bkg	30.13	6.68	10.21	11.84
Signal (M_H = 120 GeV)				
WH	0.56	0.29	0.21	0.061
ZH	0.27	0.13	0.10	0.040

III. MULTIJET AND W+JET ESTIMATION

We estimate instrumental background contribution, corresponding to the sum of multijet background and W+jet backgrounds, using three independent data samples and identical selections, except with the NN_τ requirements reversed, by requiring that either one or both τ_h candidates have $NN_\tau < 0.75$ for type 1 and 2 and $NN_\tau < 0.95$ for type 3. The simulated background is subtracted before the samples are used to determine the differential distributions and normalization of the multijet background in the signal region. A second method used to estimate the instrumental background is based on the fact that events with $Q = \pm 1$ are signal-like, whereas events with $Q = \pm 3$ correspond largely to instrumental background. The instrumental contributions are determined separately for each tau type, as the background from misidentified jets is different in each of the three categories.

Due to low statistics available to this analysis W+jet is predicted as part of the instrumental background along with the MJ as there is no suitable sample form which to reweigh the MC W+jets.

The total rate of expected instrumental background events following all selections is determined to be 6.82 $\pm$ 1.62 events.

IV. FINAL DISCRIMINANTS

To improve the discrimination of signal from background, the data are subdivided into bins of jet multiplicity. The separation in different bins of jet multiplicity increases the sensitivity to signal, as the composition of the background is different, with the 0 jet bin being dominated by background from diboson decays and the 1 jet bin sample by

TABLE II: Systematic uncertainties on the signal and background contributions for the $\tau\tau\mu$ +X channel. Systematic uncertainties are listed by name; see the original references for a detailed explanation of their meaning and on how they are derived. Shape uncertainties are labeled with the "s" designation. Cross section uncertainties on the $gg \to H$ signal depend on the jet multiplicity, as described in the main text. Uncertainties are relative, in percent, and are symmetric unless otherwise indicated.

Contribution	Dibosons	Z/γ^*	$t\bar{t}$	Instrumental	$gg \to H$	$qq \to qqH$	VH
Luminosity/Normalization	6	6	6	24	6	6	6
Trigger	3	3	3	–	3	3	3
Cross Section (Scale/PDF)	7	6	10	–	13-33/7.6-30	4.9	6.2
PDF	–	–	–	–	2.5	2.5	2.5
Tau Id per τ (Type 1/2/3)	7/3.5/5	7/3.5/5	7/3.5/5	–	7/3.5/5	7/3.5/5	7/3.5/5
Tau Energy Scale	1	1	1	–	1	1	1
Tau Track Match per τ	1.4	1.4	1.4	–	1.4	1.4	1.4
Muon Identification	2.9	2.9	2.9	–	2.9	2.9	2.9

background from $Z/\gamma^* \to \tau\tau$ production. The majority of the multijet and W+jet contribution is found in the higher jet multiplicity bins.

In Fig. 1(a) we show the transverse momentum, p_T, of the leading p_T tau and in Fig. 1(b) the p_T of the leading p_T muon. Fig. 1(c) a variable referred to as H_T is shown. This is shown to give large separation between signal and background and uses the information of the leptons p_T, the $\not{p}_T$ and the jet p_T. It is defined as

$$H_T = \sum_{i=0}^{m} p_T(i) + \not{p}_T + \sum_{j=0}^{n} p_T(j)$$

where m = the number of leptons (m=3 for this analysis) and n = the number of jets (up to two reconstructed jets are allowed in this analysis).

The expected number of background and signal events split into bins of jet multiplicity and the observed numbers of events in data are shown in Table I.

V. SYSTEMATIC UNCERTAINTIES

The uncertainties determined for this Higgs search are summarized in Table V. The theoretical uncertainty on background cross sections for $Z/\gamma^* \to \ell^+\ell^-$, W+jets, $t\bar{t}$, and diboson production vary between $6\% - 10\%$. The uncertainty on the measured integrated luminosity is 6.1% [14]. The systematic uncertainty on muon identification is 2.9% per muon and the uncertainty on the identification of τ_h, including the uncertainty from applying a neural network to discriminate τ_h from jets, is 4% for each type 1, 7% for each type 2 τ_h candidate and 5% for each type 3 τ_h candidate. The trigger efficiency has a systematic uncertainty of 3%. A uncertainty of 23.7% as derived from the statistical uncertainty arising from the determination method is applied for the multijet and W+jet determination. The error on the signal acceptance due to PDF uncertainties is taken to be 2.5%. The theoretical cross section uncertainty for the associated production (VH) signal is taken to be 6.2%, for the gluon-gluon fusion signal is taken to be 5% and for the vector boson fusion signal is taken to be 4.9%

VI. LIMITS

Since the data are well described by the background expectation, we determine limits on the SM Higgs production cross section as a ratio of the 95% C.L limits over the SM Higgs cross section. The H_T distribution is used as the discriminating variable in the limit setting procedure. A modified frequentist approach [15] is used. A log-likelihood ratio (LLR) test statistic is formed using the Poisson probabilities for estimated background yields, the signal acceptance, and the observed number of events for different SM higgs mass hypotheses. The confidence levels are derived by integrating the LLR distribution in pseudo-experiments using both the signal-plus-background (CL_{s+b}) and the background-only hypotheses (CL_b). The excluded production cross section is taken to be the cross section for which the confidence level for signal, $CL_s = CL_{s+b}/CL_b$, equals 0.05. Systematic uncertainties on both background and signal, including their correlations, are taken into account. To minimize the degrading effects of systematics on

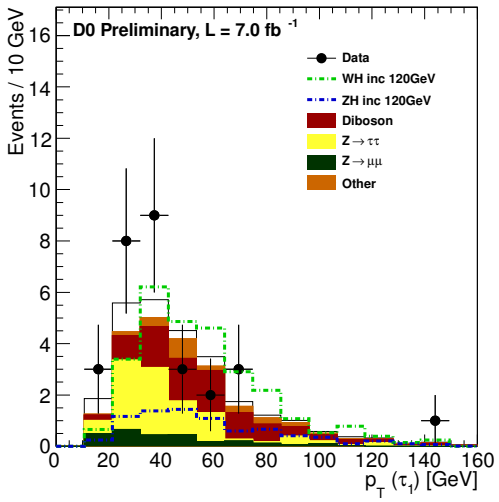

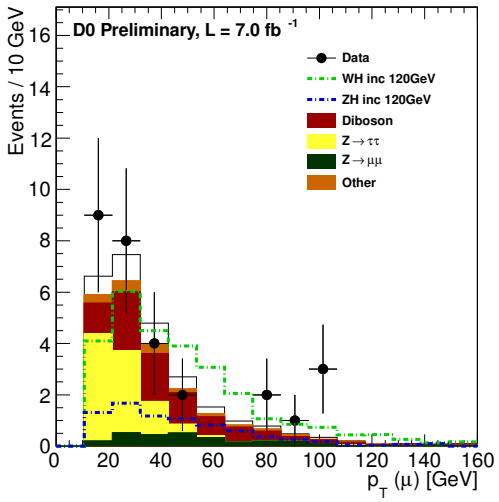

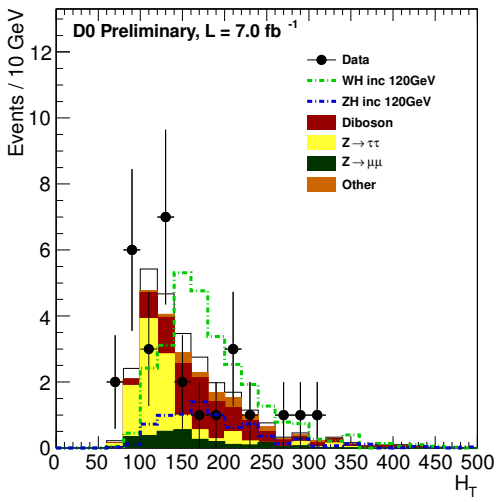

FIG. 1: The p_T distributions for the (a) leading p_T tau and (b) leading p_T muon , and (c) reconstructed transverse momentum of the SM Higgs, H_T. The data are compared to the sum of the expected background and to simulations of the signal from the associated production of a SM Higgs boson with a W and Z boson. "Other" background comprises $Z/\gamma^* \to e^+e^-$, and $t\bar{t}$ processes.

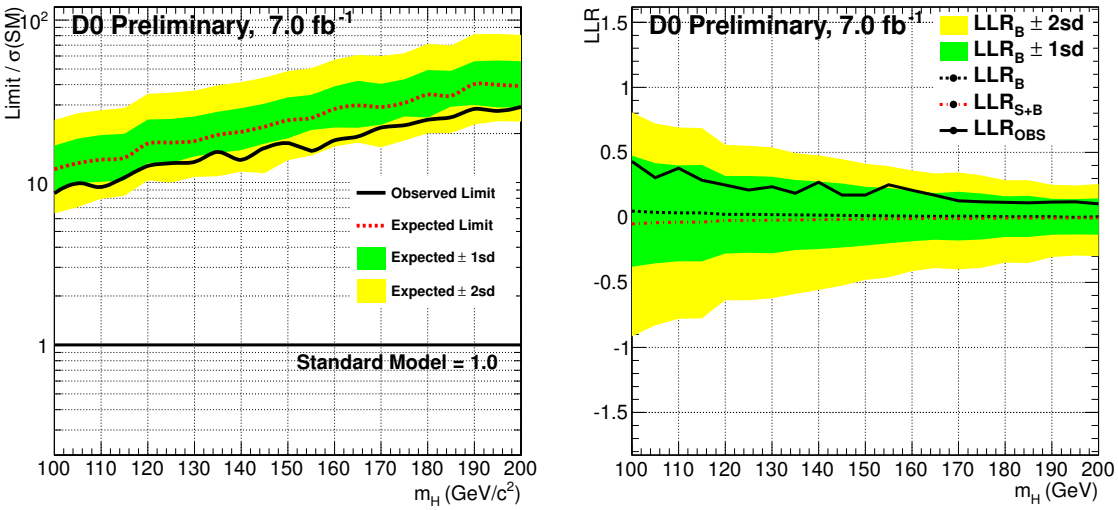

FIG. 2: Expected and observed limits at the 95% C.L show as a ratio of the determined cross section to the standard model Higgs cross section and the corresponding LLR distribution.

the search sensitivity, the background contributions are fit to the data observation by maximizing a profile likelihood function for the background-only and signal-plus-background hypotheses.

In Fig. 2, the upper limits on the determined cross section as a ratio of the SM higgs cross section are shown and the numerical values are given in Table III.

TABLE III: Expected and observed combined cross section limits at 95% C.L for different Higgs masses. This was calculated using data corresponding to 7.0 fb^{-1} of integrated luminosity and evaluated using the `CLfit2` method .

Limits / Mass (GeV)	100	105	110	115	120	125	130	135	140	145	150
$\sigma_{exp}/\sigma_{exp}(SM)$	12.1	13.2	13.8	14.2	17.4	17.6	18.0	19.7	20.5	22.1	24.2
$\sigma_{obs}/\sigma_{obs}(SM)$	8.6	9.9	9.4	10.7	12.6	13.1	13.4	15.4	13.8	16.3	17.5

Limits / Mass (GeV)	155	160	165	170	175	180	185	190	195	200
$\sigma_{exp}/\sigma_{exp}(SM)$	24.9	28.4	29.8	29.1	30.9	34.8	34.2	40.3	39.9	39.2
$\sigma_{obs}/\sigma_{obs}(SM)$	15.6	18.2	19.2	21.8	22.5	24.4	25.2	28.3	27.6	29.2

VII. SUMMARY

A new search for the standard model Higgs boson decaying into μ and τ leptons is presented. This was performed using Tevatron Run II data corresponding to 7 fb $^{-1}$. At least one muon and two taus where required in the final state. No evidence for a SM Higgs boson was seen so limits were placed on the ratio of the cross section to the standard model Higgs cross section.

We thank the staffs at Fermilab and collaborating institutions, and acknowledge support from the DOE and NSF (USA); CEA and CNRS/IN2P3 (France); FASI, Rosatom and RFBR (Russia); CNPq, FAPERJ, FAPESP and FUNDUNESP (Brazil); DAE and DST (India); Colciencias (Colombia); CONACyT (Mexico); KRF and KOSEF (Korea); CONICET and UBACyT (Argentina); FOM (The Netherlands); STFC and the Royal Society (United Kingdom); MSMT and GACR (Czech Republic); CRC Program and NSERC (Canada); BMBF and DFG (Germany);

SFI (Ireland); The Swedish Research Council (Sweden); and CAS and CNSF (China).

---

[1] LEP Electroweak Working Group, (2011) http://lepewwg.web.cern.ch/LEPEWWG/

[2] [TEVNPH (Tevatron New Phenomina and Higgs Working Group) and CDF and D0 Collaborations], arXiv:1107.5518 [hep-ex]. (2011)

[3] The CSM collaboration, Combination of CMS searches for a Standard Model Higgs boson, CMS PAS HIG-11-03 (2011) http://cdsweb.cern.ch/record/1406347/files/HIG-11-032-pas.pdf

[4] The ATLAS collaboration, Combination of Higgs Boson Searches with up to 4.9 fb-1 of pp Collisions Data Taken at a center-of-mass energy of 7 TeV with the ATLAS Experiment at the LHC, ATLAS-CONF-2011-163 (2011) http://cdsweb.cern.ch/record/1406358

[5] J. Kraus, C. McGivern DØ Note **6276** (2012).

[6] V.M. Abazov *et al.* (D0 Collaboration), Nucl. Instrum. Methods Phys. Res. A **565**, 463 (2006); M. Abolins *et al.*, Nucl. Instrum. Methods in Phys. Res. A **584**, 75 (2008); R. Angstadt *et al.*, Nucl. Instrum. Methods in Phys. Res. A **622**, 298 (2010).

[7] M.L. Mangano et al., J. High Energy Physics **07**, 001 (2003).

[8] T. Sjöstrand *et al.*, Comput. Phys. Commun. **135**, 238 (2001).

[9] A. Djouadi, J. Kalinowski and M. Spira, Comput. Phys. Commun. **108**, 56 (1998) [hep-ph/9704448].

[10] Z. Was, Nucl.Phys.Proc.Suppl., **98**, 96 (2001).

[11] R. Brun and F. Carminati, CERN Program Library Long Writeup W5013, 1993.

[12] V.M. Abazov *et al.* (D0 Collaboration), Phys. Rev. D **71**, 072004 (2005); erratum-ibid. D **77**, 039901 (2008).

[13] The pseudorapidity is defined as $\eta = -\ln[\tan(\theta/2)]$, where θ is the polar angle with respect to the proton beam direction.

[14] T. Andeen *et al.*, FERMILAB-TM-2365 (2007).

[15] W. Fisher, FERMILAB-TM-2386-E (2006).